

Amplitude Estimation without Phase Estimation

Yohichi Suzuki^{1,+}, Shumpei Uno^{1,2,+}, Rudy Raymond^{1,3}, Tomoki Tanaka^{1,4}, Tamiya Onodera^{1,3}, and Naoki Yamamoto^{1,*}

¹Quantum Computing Center, Keio University, 3-14-1 Hiyoshi, Kohoku-ku, Yokohama, Kanagawa, 223-8522, Japan

²Mizuho Information & Research Institute, Inc., 2-3 Kanda-Nishikicho, Chiyoda-ku, Tokyo, 101-8443, Japan

³IBM Research - Tokyo, 19-21 Nihonbashi Hakozaki-cho, Chuo-ku, Tokyo, 103-8510, Japan

⁴Mitsubishi UFJ Financial Group, Inc. and MUFG Bank, Ltd., 2-7-1 Marunouchi, Chiyoda-ku, Tokyo, 100-8388, Japan

⁺these authors equally contributed to this work

^{*}yamamoto@appi.keio.ac.jp

November 10, 2021

Abstract

This paper focuses on the quantum amplitude estimation algorithm, which is a core subroutine in quantum computation for various applications. The conventional approach for amplitude estimation is to use the phase estimation algorithm which consists of many controlled amplification operations followed by the quantum Fourier transform. The whole procedure is however hard to implement with current and near-term quantum computers. In this paper, we propose a quantum amplitude estimation algorithm without the use of expensive controlled operations; the key idea is to employ the maximum likelihood estimation based on the combined measurement data produced from quantum circuits with different numbers of amplitude amplification operations. Numerical simulations demonstrate that our algorithm asymptotically achieves nearly the optimal quantum speedup yet with reasonable circuit length.

1 Introduction

Quantum computers are expected to allow us to perform a high-speed computation over classical computation for problems appearing in a wide range of fields

in science and technology. In recent years, environments in which quantum algorithms can be executed by real quantum devices are being provided [1, 2, 3]. The real quantum devices with several tens of qubits are about to be realized in near future, although those are the so-called noisy intermediate-scale quantum (NISQ) devices imposing several practical limitations on their use [4], both in the number of gate operations and the number of available qubits. Hence several architectures taking into account these constraints have been proposed, typically the variational quantum eigensolver [5, 6].

This paper focuses on the amplitude estimation algorithm, which is a core subroutine in quantum computation for various applications, e.g., in chemistry [7, 8], finance [9, 10], and machine learning [11, 12, 13, 14]. In particular, quantum speedup of Monte Carlo sampling via amplitude estimation [15] lies in the heart of those applications. In light of its importance, therefore, we follow the same direction mentioned above and aim to develop a new amplitude estimation algorithm that can be executed in NISQ devices.

Here we put a remark. In Ref. [16] it was shown that the amplitude estimation problem can be formulated as a phase estimation problem [17], where the amplitude to be estimated is inferred from the eigenvalue of the corresponding amplification operator. Owing to the ubiquitous nature of eigenvalue estimation problem, there have been proposed some versions of phase estimation algorithm suitable for NISQ devices [18, 19, 20, 21], which rely on the classical post-processing statistics such as the Bayes method. However, those modified phase estimation algorithms as well as the original scheme [17] still involve many controlled operations (e.g., the controlled amplification operation in the case of Ref. [16]) that can be difficult to apply on NISQ devices. Therefore it certainly deserves devising a new algorithm specialized to the amplitude estimation problem that does not use expensive controlled operations.

The goal of amplitude estimation is, in the simplest form, to estimate the unknown parameter θ contained in the state $|\Psi\rangle = \sin \theta |\text{good}\rangle + \cos \theta |\text{bad}\rangle$, where $|\text{good}\rangle$ and $|\text{bad}\rangle$ are given orthogonal state vectors. Our scheme is composed of the amplitude amplification process and the maximum likelihood (ML) estimation; the controlled operations and the subsequent quantum Fourier transform (QFT) are not involved. The amplification process transforms the coefficient of $|\text{good}\rangle$ to $\sin((2m+1)\theta)$ with m the number of operations; if θ is known, then, by suitably choosing m , we can enhance the probability of hitting “good” quadratically greater than the classical case where no amplitude amplification is employed [22]. However, because θ is unknown in this problem, the function $\sin((2m+1)\theta)$ does not always take a relatively large value for a certain m , meaning that an effective quantum speedup is not always available; also relatively, the ML estimate is not uniquely determined due to the periodicity of this function. Our strategy is first to make measurements on the transformed quantum state and construct likelihood functions for several m , say $\{m_0, \dots, m_M\}$, and then combine them to construct a single likelihood function that uniquely produces the ML estimate; see Fig. 1. The broad concept behind this scheme is to combine the data produced from some different quantum circuits, which might be performed even on NISQ devices, to compute a target value faster than

classical algorithms via some post-processing. Actually a numerical simulation demonstrates that we can achieve nearly squared-root reduction compared to the classical random sampling in the total number of oracle calls to reach the specified estimation precision, by appropriately designing $\{m_k\}$; notably, only relatively short-depth circuits are required to have this quantum speedup. We also show that, in an application of the amplitude estimation to Monte Carlo integration, our algorithm requires much smaller number of controlled NOT (CNOT) gates, compared to the conventional phase-estimation-based approach, and thus it is suitable for obtaining quantum advantages with NISQ devices. Note that Ref. [23] also takes the approach without using the phase estimation method, but it needs changing the oracle in each iteration, which is demanding in practice.

2 Preliminary

We here briefly describe the quantum amplitude amplification which becomes the basis of our approach for the amplitude estimation problem.

Our proposed algorithm mainly consists of two parts: quantum amplitude amplification and amplitude estimation based on the likelihood analysis. The amplitude amplification [24, 25] is the generalization of the Grover's quantum searching algorithm [22]. It is known that similar to the quantum searching, the amplitude amplification achieves quadratic speedup over the corresponding classical algorithm.

We assume a unitary operator \mathcal{A} that acts on $(n + 1)$ qubits, such that $|\Psi\rangle = \mathcal{A}|0\rangle_{n+1} = \sqrt{a}|\tilde{\Psi}_1\rangle|1\rangle + \sqrt{1-a}|\tilde{\Psi}_0\rangle|0\rangle$, where $a \in [0, 1]$ is the unknown parameter to be estimated, while $|\tilde{\Psi}_1\rangle$ and $|\tilde{\Psi}_0\rangle$ are the n -qubit normalized good and bad states. The sample complexity of estimating a is counted by the number of the operations of \mathcal{A} , which is often denoted as the number of *oracle calls* for simplicity. Performing measurements on $|\Psi\rangle$ repeatedly, we can infer a from the ratio of obtaining the good and bad states, but in this case the number of oracle calls is exactly the same as the classical one.

The advantage offered by the quantum amplitude amplification is that, instead of measuring right after the single operation of \mathcal{A} , we can amplify the probability of obtaining the good state by applying the following operator:

$$\mathbf{Q} = -\mathcal{A}\mathbf{S}_0\mathcal{A}^{-1}\mathbf{S}_\chi, \quad (1)$$

where the operator \mathbf{S}_χ puts negative sign to the good state, i.e., $\mathbf{S}_\chi|\tilde{\Psi}_1\rangle|1\rangle = -|\tilde{\Psi}_1\rangle|1\rangle$, and does nothing to the bad state. Similarly, \mathbf{S}_0 puts the negative sign to the all-zero state $|0\rangle_{n+1}$, and does nothing to the other states. \mathcal{A}^{-1} is the inverse of \mathcal{A} , the operation of which requires the same sample complexity as \mathcal{A} .

By defining a parameter $\theta_a \in [0, \pi/2]$ such that $\sin^2 \theta_a = a$, we have

$$\mathcal{A}|0\rangle_{n+1} = \sin \theta_a |\tilde{\Psi}_1\rangle|1\rangle + \cos \theta_a |\tilde{\Psi}_0\rangle|0\rangle. \quad (2)$$

Brassard et al. [26] showed that repeatedly applying \mathbf{Q} for m times on $|\Psi\rangle$ results in

$$\mathbf{Q}^m |\Psi\rangle = \sin((2m+1)\theta_a) |\tilde{\Psi}_1\rangle |1\rangle + \cos((2m+1)\theta_a) |\tilde{\Psi}_0\rangle |0\rangle. \quad (3)$$

This equation represents that, after applying \mathbf{Q} for m times (with $2m$ oracle calls), we can obtain the good state with probability at least $4m^2$ times larger than that obtained from $\mathcal{A}|0\rangle_{n+1}$ for sufficiently small a . This is in contrast with having $2m$ number of measurements from $\mathcal{A}|0\rangle_{n+1}$ that only gives the good state with probability $2m$ times larger. This gives an intuition of the quadratic speedup obtained from the amplitude amplification: if we can infer the ratio of the good state after the amplitude amplification, we can estimate the value of a from the number of oracle calls required to obtain such ratio.

The popular quantum phase estimation requires a quantum circuit that implements the multiple controlled \mathbf{Q} operations, namely, Controlled- \mathbf{Q} : $|m\rangle|\Psi\rangle \rightarrow |m\rangle\mathbf{Q}^m|\Psi\rangle$. Performing the controlled operations simultaneously on consecutively many m 's and gathering the amplitude by the inverse QFT results in an accurate estimation of a [26]. However, this approach suffers from the need of many controlled gates (thus, CNOT gates) and additional ancilla qubits (the number of which is dictated by the required accuracy). Such approach can be problematic for NISQ devices.

3 Amplitude estimation without phase estimation

3.1 The algorithm

In this section, we show the quantum algorithm to estimate θ_a in Eq. (3) without using the conventional phase-estimation-based method [26]. The first stage of the algorithm is to make good or bad measurements on the quantum state $\mathbf{Q}^{m_k}|\Psi\rangle$ for a chosen set of $\{m_k\}$. Let N_k be the number of measurements (shots) and h_k be the number of measuring good states for the state $\mathbf{Q}^{m_k}|\Psi\rangle$; then, because the probability measuring the good state is $\sin^2((2m_k+1)\theta_a)$, the likelihood function representing this probabilistic event is given by

$$L_k(h_k; \theta_a) = [\sin^2((2m_k+1)\theta_a)]^{h_k} [\cos^2((2m_k+1)\theta_a)]^{N_k - h_k}. \quad (4)$$

The second stage of the algorithm is to combine the likelihood functions $L_k(h_k; \theta_a)$ for several $\{m_0, \dots, m_M\}$ to construct a single likelihood function $L(\vec{h}; \theta_a)$:

$$L(\vec{h}; \theta_a) = \prod_{k=0}^M L_k(h_k; \theta_a), \quad (5)$$

where $\vec{h} = (h_0, h_1, \dots, h_M)$. The ML estimate is defined as the value that maximizes $L(\vec{h}; \theta_a)$:

$$\hat{\theta}_a = \arg \max_{\theta_a} L(\vec{h}; \theta_a) = \arg \max_{\theta_a} \ln L(\vec{h}; \theta_a) \quad (6)$$

The whole procedure is summarized to Fig. 1. Now a and θ_a are uniquely related through $a = \sin^2 \theta_a$ in the range $0 \leq \theta_a \leq \pi/2$, and $\hat{a} := \sin^2 \hat{\theta}_a$ is the ML estimate for a ; thus in what follows $L(\vec{h}; a)$ is denoted as $L(\vec{h}; \theta_a)$. It is also noted that the random variables h_0, h_1, \dots, h_M are independent but not identically distributed since the probability distribution for obtaining h_k , i.e., $p_k(h_k; \theta_a) \propto L_k(h_k; \theta_a)$, is different for each k ; however, the set of multidimensional random variables $\vec{h} = (h_0, h_1, \dots, h_M)$ is independently generated from the identical joint probability distribution $p(\vec{h}; \theta_a) \propto L(\vec{h}; \theta_a)$.

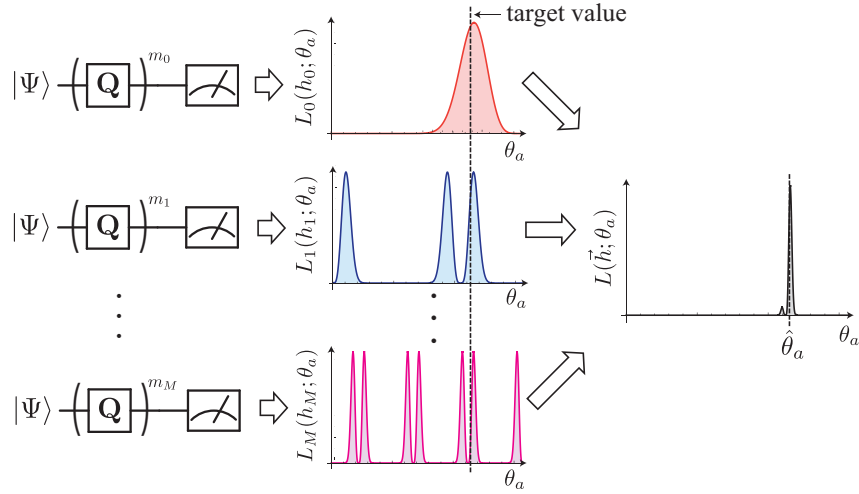


Figure 1: Schematic picture of the proposed amplitude estimation algorithm using the ML estimation.

There are two caveats on this algorithm; (i) if only a single amplitude amplification circuit is used like the Grover search algorithm, i.e., the case $M = 0$ and $m_0 \neq 0$, the ML estimate $\hat{\theta}_a$ cannot be uniquely determined due to the periodicity of $L_0(h_0; \theta_a)$, and (ii) if no amplification operator is applied, i.e., $m_k = 0 \forall k$, then the ML estimate is unique but it does not have any quantum advantages as shown later. Hence what is the heart of our algorithm can be regarded as the *quantum circuit fusion* technique that combines some quantum circuits to uniquely determine the target value while some quantum advantage is guaranteed.

3.2 Statistics; Cramér–Rao bound and Fisher information

The remaining to be determined in our algorithm is to design the sequences $\{m_k, N_k\}$, so that the resulting ML estimate $\hat{\theta}_a$ might have a distinct quantum advantage over the classical one. Here we introduce a basic statistics method to carry out this task and, based on that, give some specific choice of $\{m_k, N_k\}$.

First, in general, the *Fisher information* $\mathcal{I}(a)$ is defined as

$$\mathcal{I}(a) = \mathbb{E} \left[\left(\frac{\partial}{\partial a} \ln L(x; a) \right)^2 \right], \quad (7)$$

where the expectation is taken over a random variable x subjected to a given probability distribution $p(x; a)$ with an unknown parameter a . The importance of the Fisher information can be clearly seen from the fact that any estimate \hat{a} satisfies the following *Cramér–Rao inequality*:

$$\text{var}(\hat{a}) = \mathbb{E}[(\hat{a} - \mathbb{E}[\hat{a}])^2] \geq \frac{[1 + b'(a)]^2}{\mathcal{I}(a)}, \quad (8)$$

where $b(a)$ represents the bias defined by $b(a) = \mathbb{E}[\hat{a} - a]$ and $b'(a)$ indicates the derivative of $b(a)$ with respect to a . It is then easy to see that the mean squared estimation error satisfies

$$\mathbb{E}[(\hat{a} - a)^2] \geq \frac{[1 + b'(a)]^2}{\mathcal{I}(a)} + b(a)^2. \quad (9)$$

A specifically important property of the ML estimate, which maximizes the likelihood function $\prod_k p(x_k; a)$ with the measurement data x_k , is that it becomes unbiased, i.e., $b(a) = 0$, and further achieves the equality in Eq. (9) in the large number limit of measurements data [27]; that is, the ML estimate is asymptotically optimal.

In our case, by substituting Eqs. (4) and (5) into Eq. (7) together with a straight forward calculation $\mathbb{E}[h_k] = N_k \sin^2((2m_k + 1)\theta_a)$, we find that

$$\mathcal{I}(a) = \frac{1}{a(1-a)} \sum_{k=0}^M N_k (2m_k + 1)^2. \quad (10)$$

Also for any sequences $\{m_k, N_k\}$, the total number of oracle calls is given as

$$N_{\text{orac}} = \sum_{k=0}^M N_k (2m_k + 1). \quad (11)$$

As stated before, the coefficient 2 multiplying m_k in Eq. (11) is originated from the fact that the operator \mathbf{Q} uses \mathcal{A} and \mathcal{A}^{-1} , and the constant +1 is due to the initial state preparation of $|\Psi\rangle = \mathcal{A}|0\rangle_{n+1}$. In the case that \mathbf{Q} is not applied to $|\Psi\rangle$ and only the final measurements are performed for $|\Psi\rangle$, i.e. $m_k = 0$ for all k , the total number of the oracle calls is identical to that of classical random sampling. Since N_k and $(2m_k + 1)$ are positive integers, the Fisher information in Eq. (10) satisfies following relation:

$$\mathcal{I}(a) \leq \frac{1}{a(1-a)} \left(\sum_{k=0}^M N_k (2m_k + 1) \right)^2 = \frac{1}{a(1-a)} N_{\text{orac}}^2. \quad (12)$$

Here we set \hat{a} to be the ML estimate (6) and consider the estimation error $\hat{\epsilon} = \sqrt{\mathbb{E}[(\hat{a} - a)^2]}$ in this case. Let us now assume that the total number of measurements $\sum_{k=0}^M N_k$ is sufficiently large, in which case the ML estimate asymptotically converges to an unbiased estimate and achieves the lower bound of the Cramér–Rao inequality (8), as mentioned above. Hence, from Eqs. (8) and (12), the error $\hat{\epsilon}$ satisfies

$$\hat{\epsilon} \rightarrow \frac{1}{\mathcal{I}(a)^{1/2}} \geq \frac{\sqrt{a(1-a)}}{N_{\text{orac}}}. \quad (13)$$

(More precisely, $\hat{\epsilon} \mathcal{I}(a)^{1/2} \rightarrow 1$.) That is, the lower bound of estimation error is of the order $\mathcal{O}(N_{\text{orac}}^{-1})$, which is referred to as the Heisenberg limit. This is in stark contrast to the classical sampling method whose estimation error is lower bounded by $\sqrt{a(1-a)}/N_{\text{orac}}^{1/2}$, which is obtained by setting $m_k = 0 \forall k$ (i.e., the case with no amplitude amplification) in Eqs. (10) and (11); that is, the lower bound is at best of the order $\mathcal{O}(N_{\text{orac}}^{-1/2})$ in the classical case.

Now we can consider the problem posed at the beginning of this subsection; the problem is to design the sequences $\{m_k, N_k\}$, so that the resulting ML estimate $\hat{\theta}_a$ outperforms the classical limit $\mathcal{O}(N_{\text{orac}}^{-1/2})$ and hopefully achieves the Heisenberg limit $\mathcal{O}(N_{\text{orac}}^{-1})$, i.e., the quantum quadratic speedup. Although the problem can be formulated as a maximization problem of Fisher information (10) with respect to $\{m_k, N_k\}$ under some constraints on these variables, here we fix N_k 's to a constant and provide just two examples of the sequence $\{m_k\}$ as follows;

- Example sequence 1: $N_k = N_{\text{shot}}$ for all k , and $m_k = k$, i.e., it increases as $m_0 = 0, m_1 = 1, m_2 = 2, \dots, m_M = M$.
- Example sequence 2: $N_k = N_{\text{shot}}$ for all k , and m_k increases as $m_0 = 0, m_1 = 2^0, m_2 = 2^1, \dots, m_M = 2^{(M-1)}$.

In the case of Example sequence 1, the Fisher information (7) and the number of oracle calls (11) are calculated as $\mathcal{I}(a) = N_{\text{shot}}(2M+3)(2M+1)(M+1)/(3a(1-a))$ and $N_{\text{orac}} = N_{\text{shot}}(M+1)^2$, respectively. Since $N_{\text{orac}} \sim N_{\text{shot}}M^2$ and $\mathcal{I}(a) \sim N_{\text{shot}}M^3/(3a(1-a))$ when $M \gg 1$, the lower bound of the estimation error is evaluated as $\hat{\epsilon} = 1/\mathcal{I}(a)^{1/2} \sim N_{\text{orac}}^{-3/4}$; hence there is a distinct quantum advantage, although it does not reach the Heisenberg limit. Next for the case of Example sequence 2, we find $N_{\text{orac}} \sim N_{\text{shot}}2^{M+1}$ and $\mathcal{I}(a) \sim N_{\text{shot}}2^{2(M+1)}/3$, which as a result lead to $\hat{\epsilon} \sim N_{\text{orac}}^{-1}$. Therefore, this choice is asymptotically optimal; we again emphasize that the statistical method certainly serves as a guide for us to find an optimal sequence $\{m_k\}$ and realize an optimal quantum amplitude estimation algorithm. But note that these quantum advantages are guaranteed only in the asymptotic regime, and the realistic performance with the finite (or rather short) circuit depth should be analyzed. We will carry out a numerical simulation to see this realistic case.

3.3 Numerical simulation

In this section, the ML estimates $\hat{\theta}_a$ and errors $\hat{\epsilon}$ are evaluated numerically for several fixed target probabilities $a = \sin^2 \theta_a$. Based on the chosen sequence of $\{N_k\}$ and $\{m_k\}$ shown in the previous subsection, h_k 's in Eq. (5) are generated by the Bernoulli sampling with probability $\sin^2((2m_k + 1)\theta_a)$ for each k . The global maximum of the likelihood function can be obtained by using a modified brute-force search algorithm; the global maximum of $\prod_{k=0}^m L_k(h_k; \theta_a)$, is determined by searching around vicinity of the estimated global maximum for $\prod_{k=0}^{m-1} L_k(h_k; \theta_a)$. The errors $\hat{\epsilon}$ are evaluated by repeating the above procedures 1000 times for each N_{orac} .

In Fig. 2, the relation between the number of oracle calls and errors are plotted for the target probabilities $a = \sin^2 \theta_a = 2/3, 1/3, 1/6, 1/12, 1/24$, and $1/48$ with $N_{\text{shot}} = 100$. The (red) triangles and (black) circles in Fig. 2 are errors which are obtained by using Example sequence of 1 and 2, respectively. For comparison, the numerical simulations with $m_k = 0$ for all k are also performed and the results are plotted as (blue) squares in Fig. 2. In addition, the lower bounds of errors (13) when the estimate is not biased are also plotted as (red) dotted and (black) solid lines for Example sequence 1 and example 2, respectively. The (blue) dashed lines in Fig. 2 are the lower bounds for classical random sampling, i.e. $\sqrt{a(1-a)/N_{\text{orac}}}$.

The slopes of simulated results with the target probability $a = \sin^2 \theta_a = 1/48$ ranging from $N_{\text{orac}} \simeq 10^3$ to $N_{\text{orac}} \simeq 10^5$ in Fig. 2 are fitted by $\log \hat{\epsilon} = \gamma \cdot \log N_{\text{orac}} + \delta$, and the fitted parameters corresponding to the slope are obtained as $\gamma = -0.76$, $\gamma = -0.95$ and $\gamma = -0.50$ for Example sequences 1, 2 and classical random sampling, respectively. In the case of other target probabilities, similar slopes are obtained. The fitted values of γ for Example sequence 1 and 2 are consistent with the slopes obtained by using the Fisher information, although γ slightly deviates from the theoretical values. This slight deviation indicates that $\hat{\theta}_a$ is a biased estimate; in fact, this deviation decreases as N_{shot} increases, which is consistent with the fact that, in general, the ML estimate becomes unbiased asymptotically as the sampling number increases. Also, the efficiency of the ML estimate can be observed in the numerical simulation; that is, the estimation error approaches to the Cramér–Rao lower bound (13).

Finally, we remark that the computational cost for naively finding the maximum of the likelihood function is of the order $\mathcal{O}((1/\epsilon) \ln(1/\epsilon))$ in case where m_k exponentially grows as in Example sequence 2. This is because the computational complexity to obtain the likelihood function $\ln L(\vec{h}; \theta_a)$ is evaluated as $\mathcal{O}(M)$ in this case. The order of the error ϵ is estimated as $\mathcal{O}(N_{\text{orac}}^{-1})$ based on the Cramér–Rao bound. Since $N_{\text{orac}} \sim 2^M N_{\text{shot}}$, the complexity of evaluating the likelihood function is $\mathcal{O}(\ln(1/\epsilon))$. Assuming that the brute-force search among $1/\epsilon$ segments is performed to find global maximum of likelihood function, the complexity of finding the maximum is $\mathcal{O}((1/\epsilon) \ln(1/\epsilon))$. In summary, the computational complexity for the cases in which m_k is zero for all k (namely, the case of classical random sampling), and m_k exponentially increases (namely, the case of Example sequence 2), are given as $\mathcal{O}(1/\epsilon^2)$ and $\mathcal{O}((1/\epsilon) \ln(1/\epsilon))$,

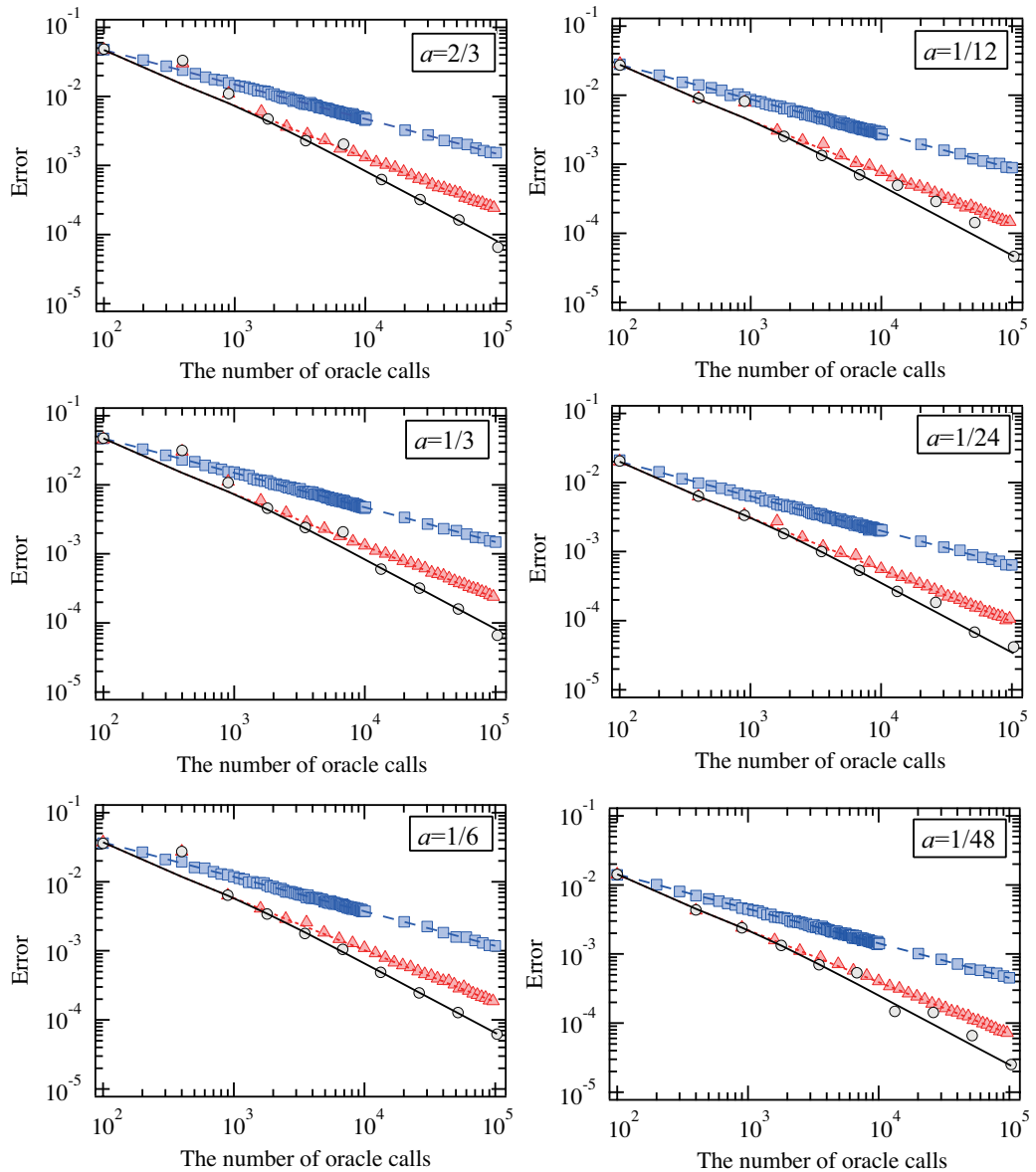


Figure 2: The relationships between the number of oracle calls and the estimation error for several target probabilities $a = \sin^2 \theta_a$.

respectively.

4 Application to the Monte Carlo integration

As an example of the application of our algorithm, the Monte Carlo integration is shown below. In this section, we first review the quantum algorithm to calculate the Monte Carlo integration by amplitude estimation [15], and then explain amplitude amplification operator used in our algorithm. Next, we present the integral of the sine function as the simple example of Monte Carlo integration. Using this example, we discuss the number of CNOT gates and qubits required for our algorithm and the conventional amplitude estimation [26].

4.1 The Monte Carlo integration as amplitude estimation

One purpose of the Monte Carlo integration is to calculate the expected value of real valued function $0 \leq f(x) \leq 1$ defined for n -bit input $x \in \{0, 1\}^n$ with probability $p(x)$:

$$\mathbb{E}[f(x)] = \sum_{x=0}^{2^n-1} p(x)f(x). \quad (14)$$

In quantum algorithm for the Monte Carlo integration, an additional (ancilla) qubit is introduced and assumed to be rotated as

$$\mathcal{R}|x\rangle_n|0\rangle = |x\rangle_n \left(\sqrt{f(x)}|1\rangle + \sqrt{1-f(x)}|0\rangle \right), \quad (15)$$

where \mathcal{R} is a unitary operator acting on $n+1$ qubits. In addition, an algorithm \mathcal{P} is introduced and operating \mathcal{P} to n -qubit register $|0\rangle_n$ yields

$$\mathcal{P}|0\rangle_n = \sum_{x=0}^{2^n-1} \sqrt{p(x)}|x\rangle_n, \quad (16)$$

where all qubits in $|0\rangle_n$ are in the state $|0\rangle$. Operating $\mathcal{R}(\mathcal{P} \otimes \mathbf{I}_1)$ to the state $|0\rangle_n|0\rangle$ generates $|\Psi\rangle$:

$$|\Psi\rangle = \mathcal{R}(\mathcal{P} \otimes \mathbf{I}_1)|0\rangle_n|0\rangle \quad (17)$$

$$= \sum_{x=0}^{2^n-1} \sqrt{p(x)}|x\rangle_n \left(\sqrt{f(x)}|1\rangle + \sqrt{1-f(x)}|0\rangle \right), \quad (18)$$

where \mathbf{I}_1 is the identity operator acting on an ancilla qubit. For convenience, we put $a = \sum_{x=0}^{2^n-1} p(x)f(x)$ and introduce two orthonormal basis:

$$|\tilde{\Psi}_1\rangle = \frac{1}{\sqrt{a}} \sum_{x=0}^{2^n-1} \sqrt{p(x)}\sqrt{f(x)}|x\rangle_n|1\rangle, \quad (19)$$

$$|\tilde{\Psi}_0\rangle = \frac{1}{\sqrt{1-a}} \sum_{x=0}^{2^n-1} \sqrt{p(x)}\sqrt{1-f(x)}|x\rangle_n|0\rangle. \quad (20)$$

By using these basis, the state $|\Psi\rangle$ can be rewritten as

$$|\Psi\rangle = \sqrt{a}|\tilde{\Psi}_1\rangle + \sqrt{1-a}|\tilde{\Psi}_0\rangle. \quad (21)$$

Then the square root of expected value $a = \mathbb{E}[f(x)]$ appears in the amplitude of $|\tilde{\Psi}_1\rangle$ and the Monte Carlo integration can be regarded as an amplitude estimation of $|\tilde{\Psi}_1\rangle$. It is known that the operator \mathbf{Q} defined in Eq. (1) can be realized by $\mathbf{U}_\Psi \mathbf{U}_{\tilde{\Psi}_0}$, where $\mathbf{U}_{\tilde{\Psi}_0} = \mathbf{I} - 2|\tilde{\Psi}_0\rangle\langle\tilde{\Psi}_0|$, $\mathbf{U}_\Psi = \mathbf{I} - 2|\Psi\rangle\langle\Psi|$, and \mathbf{I} is the identity acting on $n+1$ qubits [26]. In terms of the practical point of view, we use $\mathbf{U}_{\tilde{\Psi}_0} = \mathbf{I}_{n+1} - 2\mathbf{I}_n|0\rangle\langle 0|$, where $\mathbf{I} = \mathbf{I}_{n+1} = \mathbf{I}_n \otimes (|0\rangle\langle 0| + |1\rangle\langle 1|)$. By putting $a = \sin^2 \theta_a$, and using Eq. (3), we can apply our algorithm to the Monte Carlo integration. The circuit diagram of the amplitude amplification used in our algorithm is shown in Fig. 3. Note that the multi-qubit gate consisting of \mathcal{P} and \mathcal{R} in Fig. 3 corresponds to the quantum algorithm \mathcal{A} shown in Sec. 2, and the only ancilla qubit for each k is measured when our algorithm is applied to the Monte Carlo. Similarly, the circuit of the conventional amplitude estimation [26] is shown in Fig. 4. In the following, we apply our algorithm to very simple integral of the sine function and compare the number of CNOT gates and qubits with the result of conventional amplitude estimation.

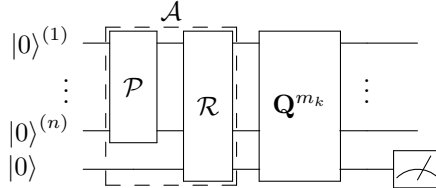


Figure 3: Quantum circuit of amplitude amplification for the Monte Carlo integration.

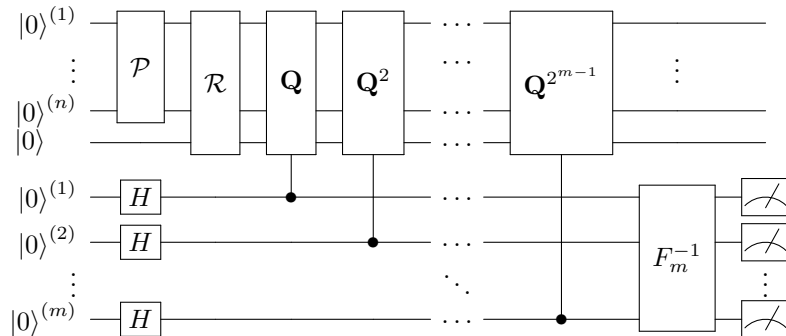


Figure 4: Quantum circuit of conventional amplitude estimation for the Monte Carlo integration. F_m^{-1} represents the inverse QFT of m qubits.

4.2 Simple example: integral of the sine function

As a simple example of the Monte Carlo integration, we consider the following integral:

$$I = \frac{1}{b_{\max}} \int_0^{b_{\max}} \sin(x)^2 dx, \quad (22)$$

where b_{\max} is a constant which determines the upper limit of the integral. By discretizing this integral in n -qubit, we obtain

$$S = \sum_{x=0}^{2^n-1} p(x) \sin^2 \left(\frac{(x + \frac{1}{2}) b_{\max}}{2^n} \right), \quad (23)$$

where $p(x) = \frac{1}{2^n}$ is a discrete uniform probability distribution. In order to apply our algorithm to calculate the sum (23), we now describe the operators \mathcal{P} and \mathcal{R} explicitly. The operator \mathcal{P} acting on the n -qubit initial state can be defined as

$$\mathcal{P} : |0\rangle_n |0\rangle \rightarrow \frac{1}{\sqrt{2^n}} \sum_{x=0}^{2^n-1} |x\rangle_n |0\rangle. \quad (24)$$

The operator \mathcal{P} can be constructed by n Hadamard gates. The operator \mathcal{R} acting on the $(n+1)$ -qubit state $|x\rangle_n |0\rangle$ can be defined as

$$\mathcal{R} : |x\rangle_n |0\rangle \rightarrow |x\rangle_n \left(\sin \left(\frac{(x + \frac{1}{2}) b_{\max}}{2^n} \right) |1\rangle + \cos \left(\frac{(x + \frac{1}{2}) b_{\max}}{2^n} \right) |0\rangle \right). \quad (25)$$

The operator \mathcal{R} can be constructed using controlled Y-rotations as illustrated in Fig. 5.

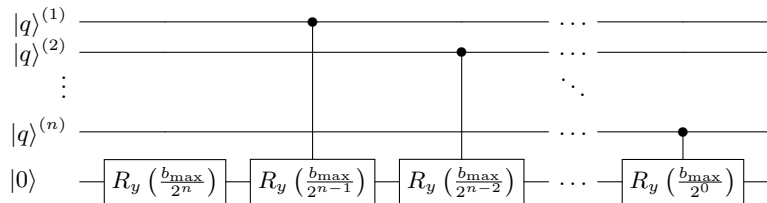


Figure 5: Quantum circuit realizing the operator \mathcal{R} in Eq. (25). In this circuit, $|x\rangle$ in Eq. (25) is represented by n qubits, denoted by $|q\rangle^{(1)}$, $|q\rangle^{(2)}$, ..., $|q\rangle^{(n)}$. $R_y(\theta)$ represents a Y-rotation with angle θ .

As an example, we now explicitly show the circuits for amplitude amplification used in our algorithm and conventional amplitude estimation with single \mathbf{Q} operation, which calculate the sum (23). For simplicity, the circuit for $b_{\max} = \pi/4$ and $n = 2$ is shown here. The quantum circuits for amplitude amplification and conventional amplitude estimation are shown in Fig. 6 and Fig. 7,

respectively. In these circuits, all-to-all qubit connectivity is assumed. From these figures, we can see that the circuit for conventional amplitude estimation tends to have more gates and qubits than that of our algorithm. Furthermore, the multi-controlled operation in the conventional amplitude estimation circuit of Fig. 7 may require several ancilla qubits.

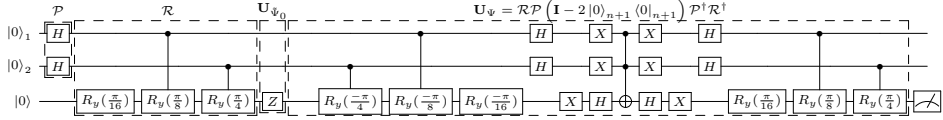


Figure 6: Quantum circuit of amplitude amplification in the case of $n = 2$ with single **Q** operation.

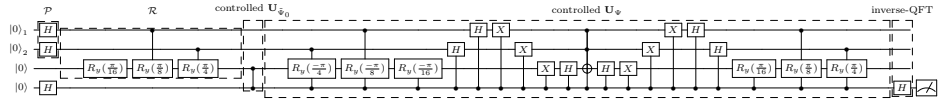


Figure 7: Quantum circuit of conventional amplitude estimation in the case of $n = 2$ with single **Q** operation.

Table 1 shows the number of CNOT gates and qubits as a function of the number of **Q** operators required for conventional amplitude estimation and our algorithm. Here we assumed the gate set supported by Qiskit ver.0.7 [28]. In this table, the number of gates in our algorithm contain only those for the circuit of the largest m_k . The numbers of CNOT gates in our algorithm is about 18 times smaller than those of conventional amplitude estimation. The number of qubits required for conventional amplitude estimation increases as the number of **Q** operations, while that for our algorithm keeps constant.

5 Conclusion

We proposed a quantum amplitude estimation algorithm achieving quantum speedup by avoiding the excessive use of controlled gates with ML estimation. The essential idea of the proposed algorithm is constructing a likelihood function using the outcomes of measurements on several quantum states, which are transformed by amplitude amplification process. Although the probability measuring good or bad states depends on the number of amplitude amplification operations, the outcomes are correlated with each other due to the fact that the each amplified probability is a function of the single parameter, which is to be estimated. To confirm the efficiency of the proposed algorithm, numerical simulations were performed, and relations between the number of oracle calls and the estimation errors were analyzed. As a result, it was shown that the proposed algorithm can estimate the target value with the smaller number of oracle calls in comparison with classical algorithm. We also discussed the lower bound of the estimation error in terms of the Fisher information, and found that the

Table 1: The number of CNOT gates and qubits to calculate (23) as a function of \mathbf{Q} operations.

| # operators \mathbf{Q} | conventional amplitude estimation | | our algorithm | |
|--------------------------|-----------------------------------|----------|---------------|----------|
| | # CNOT gates | # qubits | # CNOT gates | # qubits |
| 0 | - | - | 4 | 3 |
| 2^0 | 135 | 7 | 18 | 3 |
| 2^1 | 399 | 8 | 32 | 3 |
| 2^2 | 927 | 9 | 60 | 3 |
| 2^3 | 1981 | 10 | 116 | 3 |
| 2^4 | 4085 | 11 | 228 | 3 |
| 2^5 | 8287 | 12 | 452 | 3 |
| 2^6 | 16683 | 13 | 900 | 3 |
| 2^7 | 33465 | 14 | 1796 | 3 |
| 2^8 | 67017 | 15 | 3588 | 3 |

estimation errors observed in numerical simulation are sufficiently close to the Heisenberg limit. In addition, the proposed algorithm was applied to the Monte Carlo integration, and the number of CNOT gates and qubits were counted. As a result, it was found that the smaller number of CNOT gates and qubits is required to perform the Monte Carlo integration in comparison with the conventional amplitude estimation. These facts indicate that the proposed algorithm could work well even with the noisy intermediate-scale quantum devices.

References

- [1] IBM Q Experience. <https://quantumexperience.ng.bluemix.net/qx/editor>. Accessed: 2019-03-26.
- [2] N. Friis *et al.* Observation of entangled states of a fully controlled 20-qubit system. *Physical Review X*, 8:021012, 2018.
- [3] C. Song *et al.* 10-qubit entanglement and parallel logic operations with a superconducting circuit. *Physical Review Letters*, 119:180511, 2017.
- [4] J. Preskill. Quantum Computing in the NISQ era and beyond. *Quantum*, 2:79, 2018.
- [5] J. R. McClean *et al.* The theory of variational hybrid quantum-classical algorithms. *New Journal of Physics*, 18(2):023023, 2016.
- [6] M. H. Yung *et al.* From transistor to trapped-ion computers for quantum chemistry. *Scientific Reports*, 4:3589, 2014.
- [7] E. Knill, G. Ortiz and R. D. Somma. Optimal quantum measurements of expectation values of observables. *Physical Review A*, 75:012328, 2007.

- [8] I. Kassala *et al.* Polynomial-time quantum algorithm for the simulation of chemical dynamics. *Proceedings of the National Academy of Sciences*, 105(48):18681–18686, 2008.
- [9] P. Rebentrost, B. Gupt and T. R. Bromley. Quantum computational finance: Monte Carlo pricing of financial derivatives. *Physical Review A*, 98:022321, 2018.
- [10] S. Woerner and D. J. Egger. Quantum risk analysis. *npj Quantum Information*, 5(1):15, 2019.
- [11] N. Wiebe, A. Kapoor and K. M. Svore. Quantum algorithms for nearest-neighbor methods for supervised and unsupervised learning. *Quantum Information and Computation*, 15(3-4):316–356, 2015.
- [12] N. Wiebe, A. Kapoor and K. M. Svore. Quantum deep learning. *Quantum Information and Computation*, 16(7-8):541–587, 2016.
- [13] N. Wiebe, A. Kapoor and K. M. Svore. Quantum perceptron models. *Proceedings of the 30th International Conference on Neural Information Processing Systems*, pages 4006–4014, 2016.
- [14] I. Kerenidis *et al.* q-means: A quantum algorithm for unsupervised machine learning. *arXiv:1812.03584*, 2018.
- [15] A. Montanaro. Quantum speedup of Monte Carlo methods. *Proceedings of the Royal Society A: Mathematical, Physical and Engineering Sciences*, 471(2181):20150301, 2015.
- [16] G. Brassard *et al.* Quantum amplitude amplification and estimation. *Contemporary Mathematics Series Millennium*, 305:53–74, 2002.
- [17] A. Y. Kitaev. Quantum measurements and the Abelian stabilizer problem. *Electronic Colloquium on Computational Complexity*, 3, 1996.
- [18] K. M. Svore, M. B. Hastings and M. Freedman. Faster phase estimation. *Quantum Information and Computation*, 14(3-4):306–328, 2014.
- [19] N. Wiebe and C. Granade. Efficient Bayesian phase estimation. *Physical Review Letters*, 117:010503, 2016.
- [20] T. E. O’Brien, B. Tarasinski and B. M. Terhal. Quantum phase estimation of multiple eigenvalues for small-scale (noisy) experiments. *New Journal of Physics*, 21(2):023022, 2019.
- [21] E. van den Berg. Practical sampling schemes for quantum phase estimation. *arXiv:1902.11168*, 2019.
- [22] L. K. Grover. A fast quantum mechanical algorithm for database search. *Proceedings of 28th Annual ACM Symposium on Theory of Computing*, pages 212–219, 1996.

- [23] D. S. Abrams and C. P. Williams. Fast quantum algorithms for numerical integrals and stochastic processes. *arXiv:quant-ph/9908083*, 1999.
- [24] G. Brassard and P. Høyer. An exact quantum polynomial-time algorithm for Simon’s problem. *Proceedings of the 5th Israeli Symposium on Theory of Computing and Systems*, pages 12–23, 1997.
- [25] L. K. Grover. Quantum computers can search rapidly by using almost any transformation. *Physical Review Letters*, 80:4329–4332, 1998.
- [26] G. Brassard *et al.* Quantum amplitude amplification and estimation. *Contemporary Mathematics*, 305:53–74, 2002.
- [27] C. R. Rao. *Linear statistical inference and its applications*, volume 2. Wiley New York, 1973.
- [28] G. Aleksandrowicz *et al.* Qiskit: An open-source framework for quantum computing, 2019.

6 Acknowledgements

The authors are grateful to constructive comments made by Yutaka Shikano and Hideo Watanabe. This work is supported by MEXT, Q-LEAP.